# Magnetic excitations in the geometric frustrated multiferroic $CuCrO_2$

M. Frontzek,[1,*] J. T. Haraldsen,[2,3,4] A. Podlesnyak,[1] M. Matsuda,[1] A. D. Christianson,[1] R. S. Fishman,[4] A. S. Sefat,[4] Y. Qiu,[5,6] J. R. D. Copley,[5] S. Barilo,[7] S. V. Shiryaev,[7] and G. Ehlers[1]

[1]*Neutron Scattering Science Division, Oak Ridge National Laboratory, Oak Ridge, Tennessee 37831, USA*
[2]*Theoretical Division, Los Alamos National Laboratory, Los Alamos, New Mexico 87545, USA*
[3] *Center for Integrated Nanotechnologies, Los Alamos National Laboratory, Los Alamos, New Mexico 87545, USA*
[4]*Materials Science and Technology Division, Oak Ridge National Laboratory, Oak Ridge, Tennessee 37831, USA*
[5]*NIST Center for Neutron Research, National Institute of Standards and Technology, Gaithersburg, Maryland 20899, USA*
[6]*Department of Materials Science and Engineering, University of Maryland, College Park, Maryland, 20742, USA*
[7]*Institute of Solid State and Semiconductor Physics, Minsk 220 072, Belarus*

(Received 7 July 2011; published 28 September 2011)

In this paper detailed neutron scattering measurements of the magnetic excitation spectrum of $CuCrO_2$ in the ordered state below $T_{N1} = 24.2$ K are presented. The spectra are analyzed using a model Hamiltonian which includes intralayer exchange up to the next-next-nearest neighbor and interlayer exchange. We obtain a definite parameter set and show that exchange interaction terms beyond the next-nearest neighbor are important to describe the inelastic excitation spectrum. The magnetic ground state structure generated with our parameter set is in agreement with the structure proposed for $CuCrO_2$ from the results of single crystal diffraction experiments previously published. We argue that the role of the interlayer exchange is crucial to understand the incommensurability of the magnetic structure as well as the spin-charge coupling mechanism.

DOI: 10.1103/PhysRevB.84.094448 PACS number(s): 75.25.−j, 75.30.Ds, 75.47.Lx, 75.85.+t

## I. INTRODUCTION

Compounds which exhibit both an ordered magnetic phase and a ferroelectric phase are termed multiferroics. Especially the multiferroics where the electric polarization can be controlled with a magnetic field and vice versa are of continuing interest due to the potential applications. The most promising candidates for such controllable multiferroic have been found among the materials with inherent geometric magnetic frustration.[1]

Different mechanisms leading to spin-charge coupling that have been discussed in the literature include the magnetoelastic effect,[2] the "inverse" Dzyaloshinskii-Moriya interaction,[3,4] and electric dipole induction through hybridization of *p-d* orbitals as originally proposed by Arima.[5] Spin-charge coupling due to magnetostriction can occur in collinear commensurate magnetic structures as for instance observed in $RMn_2O_5$, where $R$ is a rare earth metal.[2] If magnetic order with nonzero chirality exists, which may be commensurate or incommensurate with the lattice, the inverse Dzyaloshinskii-Moriya (DM) interaction induces (by inversion symmetry breaking) an electric polarization component perpendicular to the spiral axis and the propagation vector.[3] Systems in which this situation is realized include $TbMnO_3$,[6–12] $MnWO_4$,[13–16] $RbFe(MoO_4)_2$,[17,18] $LiCu_2O_2$,[19–24] and $Ni_3V_2O_8$.[25–27] Spin-charge coupling through Arima's mechanism requires a proper-screw magnetic structure where the vector of the polarization is parallel to the screw axis and to the propagation vector, $CuFeO_2$ is the most prominent example.[5,28–34]

In this article we report a detailed analysis of the spin dynamics of the multiferroic system $CuCrO_2$ which has already been studied using a variety of techniques such as polarization in applied magnetic and electric fields,[35,36] electron spin resonance (ESR),[37] x-ray emission spectroscopy (XES),[38,39] single crystal x-ray diffraction,[40] neutron diffraction,[41–45] and inelastic neutron scattering.[46,47] This system is isostructural to $CuFeO_2$ and a detailed comparison of the two systems is instructive.

In contrast to $CuFeO_2$ which becomes multiferroic in an applied magnetic field[48] or through doping the Fe site with Al,[49] Ga,[50] or Rh,[51] $CuCrO_2$ enters the multiferroic state in zero field with the magnetic transition. In both compounds the magnetic structure in the multiferroic phase is an incommensurate proper-screw magnetic structure. However, the propagation vector found for $CuCrO_2$ with $\boldsymbol{\tau} = (\tau,\tau,0)$ and $\tau = 0.3298(1)$ is very close to the commensurate value. Unlike the propagation vector of $CuFeO_2$ which in comparison is very different, $\boldsymbol{\tau} = (\tau,\tau,3/2)$ with $\tau = 0.207$.[52]

## II. EXPERIMENT

A detailed account of the sample preparation was given previously.[45] The trigonal crystal structure (space group $R\bar{3}m$) with lattice parameters $a = 2.97$ Å and $c = 17.110$ Å was confirmed by x-ray powder analysis of crushed crystals. Further characterization with respect to their magnetic properties was done using a SQUID magnetometer. The obtained susceptibility curves are similar to data published previously.[36,42,44,53] Identifying the same characteristic points in the susceptibility data as Kimura *et al.*[53] the same two characteristic phase transition temperatures $T_{N1} = 24.2$ K and $T_{N2} = 23.6$ K were obtained for our samples. The Curie-Weiss fit between 148 and 287 K of the inverse susceptibility gave an asymptotic paramagnetic Curie temperature of $-200(1)$ K and an effective moment of 3.88(1) $\mu_B$ per $Cr^{3+}$ ion. Measurements of the magnetization measured along three orthogonal directions, [110], [$\bar{1}$10], and [001], are shown in Fig. 1. A phase transition at $H_{flop} \sim 5.3$ T can be seen in these data (the value is determined from the center of gravity of the peak in the derivative), in agreement with earlier reports.[36] At this phase transition the electrical polarization is flopped[36]

 

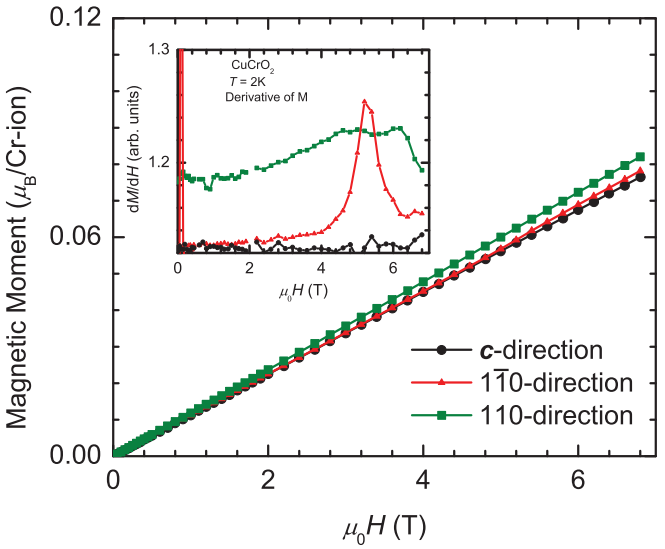


FIG. 1. (Color online) Magnetization measurement along the three main crystallographic directions in $CuCrO_2$ single crystals at $T = 2$ K. The inset shows the derivative of the magnetization with a peak at $H_{\text{flop}}$ in the $[\bar{1}10]$ direction.

in conjunction with a reorientation of the ordered magnetic moments.[44]

Ten crystals with a total mass of $m \sim 0.6$ g were co-aligned on an aluminum sheet covering an area of approximately $20 \times 20$ mm for inelastic neutron scattering experiments. The crystals were platelet like with the $c$ direction normal to the plate surface. The horizontal scattering plane was $HHL$. Experiments were conducted at the Cold Neutron Chopper Spectrometer (CNCS) at the Spallation Neutron Source in Oak Ridge,[54,55] the HB-1 triple-axis spectrometer at the High Flux Isotope Reactor in Oak Ridge, and at the Disk Chopper Spectrometer (DCS) at the NIST Center for Neutron Research (NCNR).[56]

All experiments used a standard orange cryostat in a temperature range from 1.5 to ~100 K. The CNCS measurements were performed in two settings with different incident neutron energies, 12.1 and 3 meV, respectively. The energy resolution at the elastic line was 0.4350(6) meV full width at half maximum (FWHM) at 12.1 meV and 0.0649(1) meV FWHM at 3 meV, respectively. The HB-1 measurements used constant $k_f = 14.7$ meV which resulted in an effective energy resolution of 1.84 meV at 7.5 meV. The collimation was 48-60-60-240 with two additional pyrolitic graphite (PG) filters to suppress higher order contamination. The DCS measurement was performed with an incident energy of 3.53 meV with a measured resolution of 0.1 meV (FWHM) at the elastic line. The data obtained on CNCS and DCS have been reduced using the DAVE software package.[57]

## III. THEORY

The hexagonal symmetry of the $CuCrO_2$ lattice provides a complex network of possible intra- and interlayer superexchange pathways[58] that are described by the

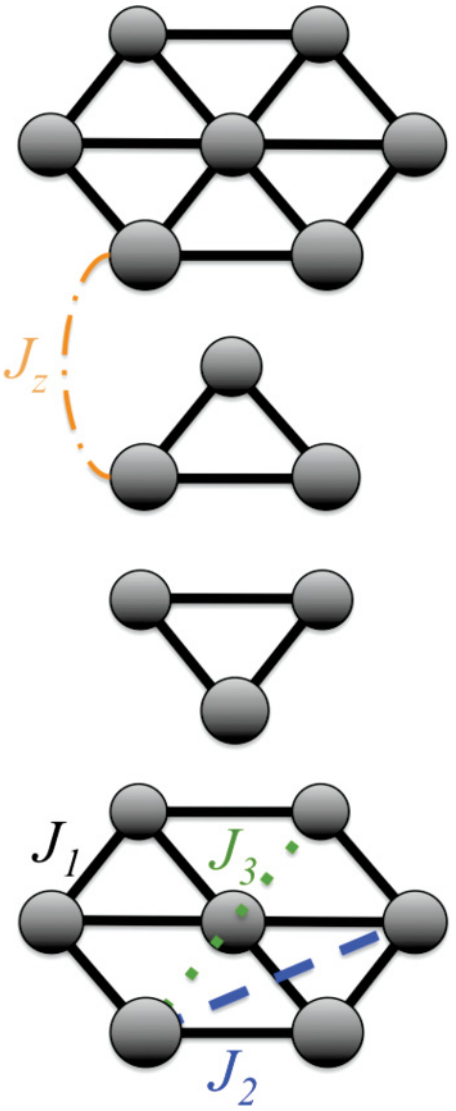


FIG. 2. (Color online) Considered exchange paths in the Heisenberg Hamiltonian.

Heisenberg Hamiltonian

$$H = -\frac{1}{2}\sum_{i\neq j} J_{ij}\mathbf{S}_i \cdot \mathbf{S}_j - D_x \sum_i \mathbf{S}_{ix}^2 - D_z \sum_i \mathbf{S}_{iz}^2, \quad (1)$$

where $\mathbf{S}_i$ is the local moment on site $i$. The superexchange interactions $J_{ij}$ between sites $i$ and $j$ are antiferromagnetic when $J_{ij} < 0$. An overview of the exchange paths in respect to the lattice is given in Fig. 2. The single-ion anisotropy along the $x$ and $z$ axes is given by $D_{x,z}$, where $D > 0$ produces easy-axis anisotropy and $D < 0$ produces easy-plane anisotropy, respectively. The three-dimensional magnetic state is constructed by stacking the two-dimensional configurations ferromagnetically along the $c$ axis.

Through an energy minimization of the exchange parameters and anisotropy, the magnetic ground state configuration is

determined through a classical approach described in Ref. 59 by defining $S_z$ within any hexagonal plane as

$$S_z(\mathbf{R}) = A \sum_{l=0} C_{2l+1} \cos[\tau_x(2l+1)x], \tag{2}$$

where the $C_{2l+1}$ harmonics are produced by the easy axis anisotropy $D_z$. With $C_1$ set to 1, the amplitude $A$ is obtained from the condition that the maximum value of $|S_z(\mathbf{R})|$ equals $S$. The perpendicular spin components $S_y$ are given by

$$S_y(\mathbf{R}) = \sqrt{S - S_z(\mathbf{R})^2}\,\mathrm{sgn}[\sin(\tau_x x)]. \tag{3}$$

The ordering wave vector $\tau_x$ and coefficients $C_{2l+1}$ are determined by minimizing the energy on a large unit cell of size $\sim 10^4 a \times a \times c$, where $a$ is the lattice constant within a hexagonal plane and $c$ is the separation between neighboring planes.

Based on this magnetic ground state, the spin dynamics are evaluated using a Holstein-Primakoff transformation, where the spin operators are given by $S_{iz} = S - a_i^\dagger a_i$, $S_{i+} = \sqrt{2S}a_i$, and $S_{i-} = \sqrt{2S}a_i^\dagger$ ($a_i$ and $a_i^\dagger$ are boson destruction and creation operators). A rotation of the local spin operators accounts for the noncollinearity of the spins.[60,61]

To determine the spin wave (SW) frequencies $\omega_{\mathbf{Q}}$, we solve the equation-of-motion for the vectors $\mathbf{v_Q} = [a_{\mathbf{Q}}^{(1)}, a_{\mathbf{Q}}^{(1)\dagger}, a_{\mathbf{Q}}^{(2)}, a_{\mathbf{Q}}^{(2)\dagger}, \ldots]$, which may be written in terms of the $2N \times 2N$ matrix $\underline{M}(\mathbf{Q})$ as $id\mathbf{v_Q}/dt = -[\underline{H}_2, \mathbf{v_Q}] = \underline{M}(\mathbf{Q})\mathbf{v_Q}$, where $N$ is the number of spin sites in the unit cell.[60] The SW frequencies are then determined from the condition $\mathrm{Det}[\underline{M}(\mathbf{Q}) - \omega_{\mathbf{Q}}\underline{I}] = 0$. To assure the local stability of a magnetic phase, all SW frequencies must be real and positive and all SW weights must be positive.

The SW intensities or weights are coefficients of the spin-spin correlation function:

$$S(\mathbf{Q},\omega) = \sum_{\alpha\beta} (\delta_{\alpha\beta} - Q_\alpha Q_\beta) S^{\alpha\beta}(\mathbf{Q},\omega), \tag{4}$$

where $\alpha$ and $\beta$ are $x$, $y$, or $z$.[61] A more detailed discussion of this method is contained in Ref. 60. Notice that magnetic neutron scattering measurements (INS) only detect components of the spin fluctuations perpendicular to the wave vector $\mathbf{Q}$. The total intensity $I(\mathbf{Q},\omega)$ for an INS scan at constant $\mathbf{Q}$ is given by

$$I(\mathbf{Q},\omega) = S(\mathbf{Q},\omega) F_{\mathbf{Q}}^2 \exp[-(\omega - \omega_{\mathbf{Q}})^2/2\delta^2], \tag{5}$$

where $\delta$ is the energy resolution and $F_{\mathbf{Q}}$ is the $Cr^{3+}$ magnetic form factor.

This approach yields additional information on the magnetic ground state. The magnetic ground state is not provided for these systems and must therefore be derived from the energy minimization of the Hamiltonian possible magnetic structures within the $\sim 10^4 a \times a \times c$ cell. Therefore, two energetically degenerate states, for instance commensurate vs slightly incommensurate, can be distinguished.

## IV. RESULTS

The inelastic excitation spectrum of $CuCrO_2$ in the $HH$ direction as measured at CNCS with $E_i = 12$ meV is shown in the upper panel of Fig. 3. Integration along the $L$ direction was in the range $0 < L < 5$ r.l.u. (relative lattice units) which is justified by a rather small dispersion along this direction. Integration along the perpendicular $H\overline{H}$ direction was within $\pm 0.025$ r.l.u. (corresponding to $\pm 2.5$ deg out of the scattering plane). For comparison the model calculation is shown in the lower panel.

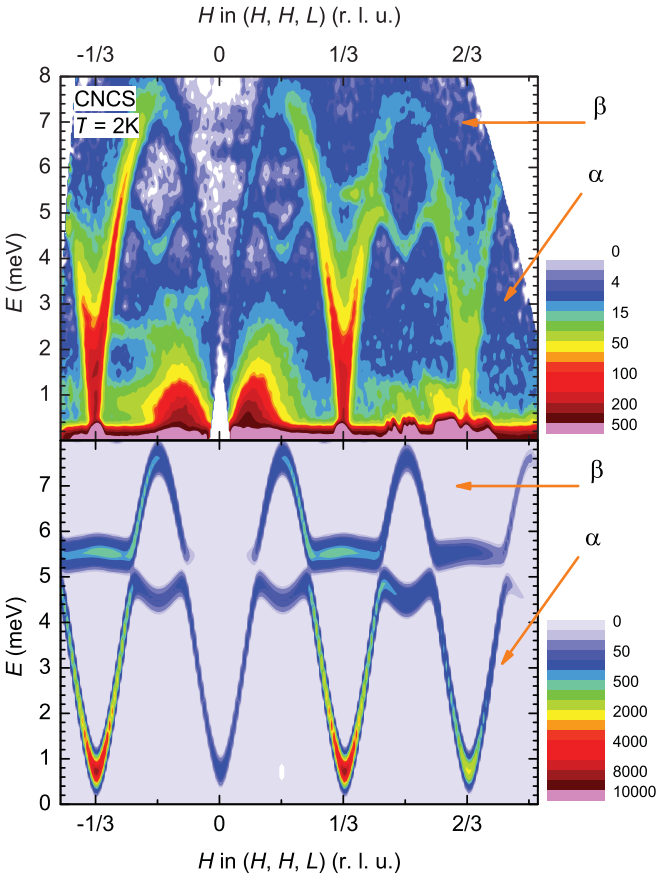


FIG. 3. (Color online) Upper panel: Magnetic excitation spectrum in $S(\mathbf{Q},\omega)$ of $CuCrO_2$ measured at $T = 2$ K at CNCS. Integration range along $L$ was from 0 to 5 in r.l.u., and along the $H\overline{H}$ direction $\pm 0.025$ r.l.u. The intensity around $H = 0$ at low energy originates from the halo of the primary beam. Lower panel: Spin waves computed from the best theoretical model, the modes discussed in the text are marked $\alpha$, $\beta$.

The low energy mode $\alpha$ originates from the magnetic Bragg peak in the vicinity of $H = 1/3$ and flattens off at around 5 meV. It has a cusp like local energy minimum at the magnetic zone boundary at $H = 1/6$. The intensity of this mode is strongest in the vicinity of the Bragg peak and falls off toward the zone boundary. This mode is mainly influenced by the model parameters $J_2$, $J_3$, $D_x$, and $D_z$ (see above). The minimum of the $\alpha$ mode at $H = 1/6$ is of considerable interest. It can only be modeled with the inclusion of an antiferromagnetic next-next nearest neighbor exchange interaction $J_3$. If $J_3$ is neglected or ferromagnetic, the excitation would be flat at $H = 1/6$ or would show a local maximum. Analyzing the intensity of the $\alpha$ mode at the zone boundary, the measurement shows more intensity at $H = 1/2$ than at $H = 1/6$. In the modeling this leads to a negative in-plane anisotropy constant $D_x$ (otherwise the intensity would

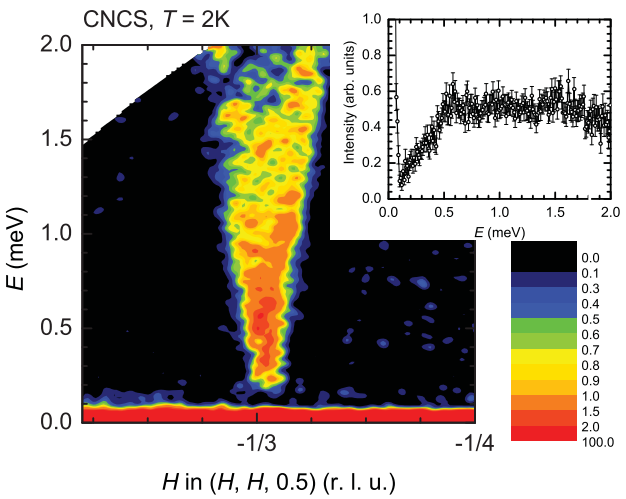


FIG. 4. (Color online) Magnetic excitation spectrum of $CuCrO_2$ measured at $T = 2$ K at CNCS with 3 meV incident energy. The inset shows a constant-$Q$ cut along the excitation. Error bars represent $\pm 1\sigma$ from counting statistics.

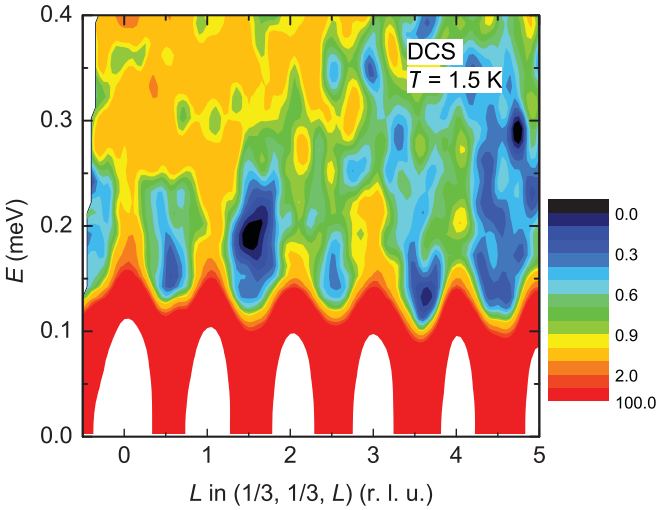


FIG. 5. (Color online) Magnetic excitation spectrum in $S(Q,\omega)$ of $CuCrO_2$ measured at $T = 2$ K at DCS with 3.55 meV incident energy. The data is integrated in the $HH$ of 0.32 to 0.34 r.l.u. from the central detector bank. The intensity is color coded in a linear scale with the exception of the elastic Bragg peaks with two orders of magnitude higher intensity.

be higher at $H = 1/6$). In return, this leads to a ground state with a proper-screw magnetic structure rather than a cycloid.

The nonzero anisotropy terms $D_x$ and $D_z$ mean that the $\alpha$ mode must be gapped. The gap is too small to be unambiguously detected at $E_i = 12.1$ meV. However, with improved energy resolution ($E_i = 3$ meV) a gap of $\sim$0.5 meV is clearly seen as shown in Fig. 4. Here the integration along the $L$ direction is only for a small range around $L = 1$. The absolute values of $D_x$ and $D_z$ are adapted in the theoretical calculations to accurately model this gap.

An overall weaker and flat $\beta$ mode is observed between 5 and 8 meV. The measurement did not resolve whether a crossing of the $\alpha$ and $\beta$ mode occurs as suggested by the calculation, mainly due to insufficient resolution. The $\beta$ mode has a maximum of $\sim$7.5 meV at the magnetic zone boundaries at $H = 1/6$ and $H = 1/2$. The energy of the $\beta$ mode at these points is mainly determined by $J_2$ and to a lesser degree by $J_3$. Kajimoto *et al.*[46] ascribed the $\beta$ mode (referred to as "flat component") to the existence of an interlayer exchange interaction $J_z$ which is inconsistent with our data. In the lower panel of Fig. 3, the computed spin wave excitation spectrum from the best theoretical model is shown. The $\alpha$ and $\beta$ mode in this energy range determine $J_2$ and $J_3$ as well as $J_1$ to which all parameters are relative. In agreement with data from the literature,[46,47] a survival of magnetic collective dynamics up to several times $T_N$ is observed at the position of the $\alpha$ mode.

The spin-wave spectrum along the $L$ direction is dispersionless for energies above 0.5 meV as already mentioned above. However, below the energy gap of 0.5 meV a modulation can be seen (Fig. 5). For an energy transfer of 0.2 meV, the measured intensity along $L$ is higher at the position of the magnetic Bragg peaks compared to the position between. This intensity pattern can be reproduced with the introduction of a ferromagnetic interlayer coupling $J_z$. The magnitude of the interlayer exchange is small as is the effect on the excitation spectrum.

The data presented so far allow the determination of the values for the exchange interaction and the anisotropy terms within the given model. The calculations replicate satisfactorily the $\alpha$ and $\beta$ excitation modes as shown in the lower panel of Fig. 3. The intensity pattern of the DCS measurement (Fig. 5) is modeled with the small interaction term $J_z$. The interlayer exchange $J_z$ also results in the magnetic ground state with the incommensurate ordering wave vector $\tau_x = 0.329$. Without the interlayer exchange the magnetic ground state would be commensurate. The model Hamiltonian also reproduces the gap in the excitation spectrum, using the anisotropy terms, which as a consequence leads to the splitting of the otherwise degenerated magnetic ground state. This splitting of the degenerate ground state gives rise to another excited state $\beta'$ at higher energies, with a spin wave dispersion that mirrors the $\beta$ mode from the ground state but which has an additional gap of 2.2 meV. The intensity of this mode is weaker than the excitations from the ground state and cannot be seen in the CNCS data, likely because, by way of how the $(\mathbf{Q},\omega)$ space is mapped in a time-of-flight measurement with the chosen settings, only $L > 1$ is covered at $\hbar\omega \gtrsim 8$ meV.

Figure 6 shows a contour map of the measurements taken at HB-1. These are constant-$E$ scans with an energy difference of 0.5 meV in the range from 1.5 to 15 meV. The measurements are along the $(HH2)$ direction. In Fig. 6 it can be seen that another mode with nearly the same dispersion exists above the $\beta$ mode, which we identify with the $\beta'$ mode resulting from the calculations. The coarser energy resolution of HB-1 leads to a partial blur of the $\beta$ and $\beta'$ mode. The calculation yields a gap between both modes of 2.2 meV at the zone boundary.

To summarize the results, the intensity and dispersion of experimentally observed spin-wave modes in $CuCrO_2$ have been modeled with a Hamiltonian that includes at least six free parameters, which are given in Table I.

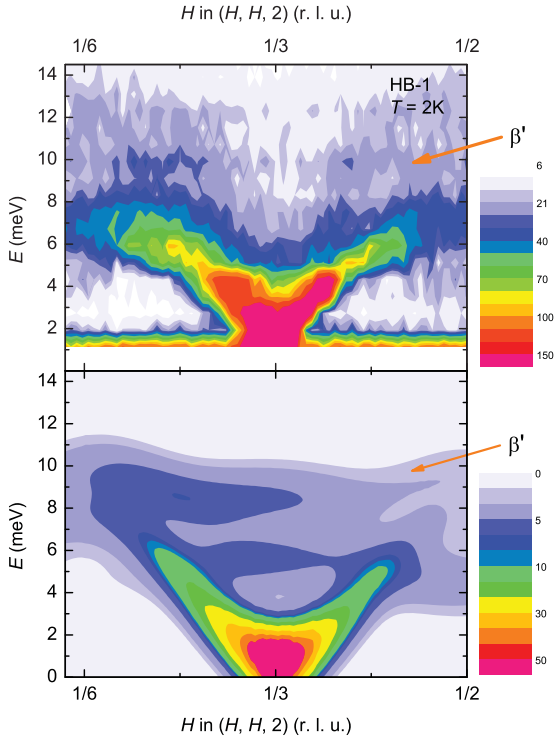


FIG. 6. (Color online) Upper panel: Contour map from constant-$E$ scans of $CuCrO_2$ measured at $T = 2$ K at HB-1. Lower panel: The corresponding model of the $\alpha$, $\beta$, and $\beta'$ excitations.

Small discrepancies between calculation and measurement suggest the need to include higher order parameters beyond the ones used here. This is most apparent in the slight discrepancy of the spin-wave velocities. The velocities depend in a nontrivial way from all interactions and deviations from the model may indicate the need for magnetoelastic or biquadratic terms. While the addition of $J_3$ and $D_z$ helps reduce this difference, it is clear that other interactions may be affecting the system. The deduction of the parameters in the Hamiltonian has been based on the approach to incorporate the least necessary number to describe the excitation spectrum satisfactorily.

In comparison to $CuFeO_2$, the nearest neighbor intralayer exchange interaction $J_1$ is one order of magnitude stronger in $CuCrO_2$, but the interlayer exchange and the anisotropy parameter $D_z$ are of comparable magnitude.[62] The different magnetic ground states are explainable with the different ratio of $D/|J_1|$. In $CuCrO_2$, where this ratio is small, the proper screw is the stable magnetic structure, while in $CuFeO_2$ the four-sublattice collinear structure is the ground state.[59,63] It has been interpreted that the main effect of doping in $CuFeO_2$ is the decrease of anisotropy and through this the proper-screw magnetic structure can be stabilized as ground state in the doped compounds.[50] Notably is the difference of the in-plane anisotropy $D_x$ which is absent in $CuFeO_2$ where a Goldstone mode at the incommensurate wave vector is observed,[58] but present in $CuCrO_2$ as indicated by the gap of the $\alpha$ mode. Instead of $D_x$ the observed lattice distortion in the basal plane is relevant to model the excitation spectra in $CuFeO_2$.[62]

TABLE I. Comparison of the relevant exchange interaction and anisotropy parameters from Ref. 47 ($*$ only one value was fitted) with this work and the results for $CuFeO_2$ from Ref. 58 ($\dagger J_{z1}$). Energies are in meV.

| Set | $J_1$ | $J_2$ | $J_3$ | $J_z$ | $D_x$ | $D_z$ |
|---|---|---|---|---|---|---|
| Ref. 47 | −2.3 | −0.12 | – | – | −0.4* | 0.4* |
| This work | −2.8 | −0.48 | −0.08 | 0.02 | −0.59 | 0.48 |
| $CuFeO_2$ | −0.23 | −0.12 | −0.16 | −0.06† | – | 0.22 |

The interlayer exchange in $CuFeO_2$ leads to a 10-sublattice stacking sequence along the $c$ direction and can be modeled with one ferromagnetic and two antiferromagnetic exchange parameters.[58] The interlayer exchange in $CuCrO_2$ seems simpler and can be described with one ferromagnetic parameter of similar magnitude. In $CuFeO_2$ the interlayer exchange has been the most affected parameter by doping[62] which might explain the difference between $CuCrO_2$ and $CuFeO_2$.

The last marked difference to be discussed is the apparent absence of a structural phase transition in $CuCrO_2$. Strain measurements on $CuCrO_2$[40] indicate strong magnetoelastic coupling, but apparently insufficient to lead to a phase transition as in $CuFeO_2$. In the latter, it has been demonstrated that the inclusion of biquadratic terms in the Hamiltonian are relevant in the prediction of the phase diagram.[64] In $CuCrO_2$, the biquadratic terms seem less relevant for the understanding of the magnetic ground state but probably cause the slight discrepancy of the spin-wave velocities between model and experiment.

## V. CONCLUSION

A detailed investigation of the magnetic excitation spectrum of $CuCrO_2$ at low temperatures has been performed using neutron scattering techniques. The excitation spectrum has been used to deduce the relevant exchange interaction and anisotropy parameters. The parameter set points to a ground state with an incommensurate proper-screw magnetic structure in agreement with results published earlier.[42,45,47] Antiferromagnetic intralayer exchange has to be considered up to next-next nearest neighbor in order to be consistent with the experimental data.

We have also shown that interlayer exchange is relevant for $CuCrO_2$ which can thus no longer be considered as a quasi-two-dimensional system. The multiferroic properties of $CuCrO_2$ have been explained within the light of the Arima model which does not consider order between the spiral planes. It is an interesting question in which way the interlayer exchange interaction in $CuCrO_2$ affects its multiferroic properties.

## ACKNOWLEDGMENTS

We acknowledge the technical and scientific support from the staff at SNS, HFIR, and NIST. This research was sponsored by the U.S. Department of Energy, Office of Basic Energy Sciences, Materials Sciences and Engineering Division. This work utilized facilities supported in part by the National Science Foundation under Agreement No. DMR-0944772. Research at Oak Ridge National Laboratory's Spallation Neutron Source was supported by the Scientific User Facilities Division, Office of Basic Energy Sciences,

US Department of Energy. Some theoretical aspects of this work has been supported by the Center for Integrated Nanotechnologies, a US Department of Energy, Office of Basic Energy Sciences user facility. Los Alamos National Laboratory is operated by Los Alamos National Security, LLC, for the National Nuclear Security Administration of the US Department of Energy under Contract DE-AC52-06NA25396. The work in Minsk was supported in part by Belarusian Fund for Basic Scientific Research, Grant No. F10R-154.

*Corresponding author: frontzekmd@ornl.gov

[1] S.-W. Cheong and M. Mostovoy, Nat. Mater. **6**, 13 (2007).
[2] L. C. Chapon, P. G. Radaelli, G. R. Blake, S. Park, and S.-W. Cheong, Phys. Rev. Lett. **96**, 097601 (2006).
[3] H. Katsura, N. Nagaosa, and A. V. Balatsky, Phys. Rev. Lett. **95**, 057205 (2005).
[4] M. Mochizuki and N. Furukawa, Phys. Rev. Lett. **105**, 187601 (2010).
[5] T. Arima, J. Phys. Soc. Jpn. **76**, 073702 (2007).
[6] M. Kenzelmann, A. B. Harris, S. Jonas, C. Broholm, J. Schefer, S. B. Kim, C. L. Zhang, S.-W. Cheong, O. P. Vajk, and J. W. Lynn, Phys. Rev. Lett. **95**, 087206 (2005).
[7] Y. Takahashi, N. Kida, Y. Yamasaki, J. Fujioka, T. Arima, R. Shimano, S. Miyahara, M. Mochizuki, N. Furukawa, and Y. Tokura, Phys. Rev. Lett. **101**, 187201 (2008).
[8] S. B. Wilkins, T. R. Forrest, T. A. W. Beale, S. R. Bland, H. C. Walker, D. Mannix, F. Yakhou, D. Prabhakaran, A. T. Boothroyd, J. P. Hill, P. D. Hatton, and D. F. McMorrow, Phys. Rev. Lett. **103**, 207602 (2009).
[9] N. Aliouane, K. Schmalzl, D. Senff, A. Maljuk, K. Prokes, M. Braden, and D. N. Argyriou, Phys. Rev. Lett. **102**, 207205 (2009).
[10] R. Kajimoto, H. Sagayama, K. Sasai, T. Fukuda, S. Tsutsui, T. Arima, K. Hirota, Y. Mitsui, H. Yoshizawa, A. Q. R. Baron, Y. Yamasaki, and Y. Tokura, Phys. Rev. Lett. **102**, 247602 (2009).
[11] F. Fabrizi, H. C. Walker, L. Paolasini, F. de Bergevin, A. T. Boothroyd, D. Prabhakaran, and D. F. McMorrow, Phys. Rev. Lett. **102**, 237205 (2009).
[12] A. M. Shuvaev, V. D. Travkin, V. Y. Ivanov, A. A. Mukhin, and A. Pimenov, Phys. Rev. Lett. **104**, 097202 (2010).
[13] G. Lautenschläger, H. Weitzel, T. Vogt, R. Hock, A. Böhm, M. Bonnet, and H. Fuess, Phys. Rev. B **48**, 6087 (1993).
[14] K. Taniguchi, N. Abe, H. Umetsu, H. A. Katori, and T. Arima, Phys. Rev. Lett. **101**, 207205 (2008).
[15] K. Taniguchi, N. Abe, S. Ohtani, and T. Arima, Phys. Rev. Lett. **102**, 147201 (2009).
[16] K. V. Shanavas, D. Choudhury, I. Dasgupta, S. M. Sharma, and D. D. Sarma, Phys. Rev. B **81**, 212406 (2010).
[17] S. A. Klimin, M. N. Popova, B. N. Mavrin, P. H. M. van Loosdrecht, L. E. Svistov, A. I. Smirnov, L. A. Prozorova, H.-A. K. von Nidda, Z. Seidov, A. Loidl, A. Y. Shapiro, and L. N. Demianets, Phys. Rev. B **68**, 174408 (2003).
[18] M. Kenzelmann, G. Lawes, A. B. Harris, G. Gasparovic, C. Broholm, A. P. Ramirez, G. A. Jorge, M. Jaime, S. Park, Q. Huang, A. Y. Shapiro, and L. A. Demianets, Phys. Rev. Lett. **98**, 267205 (2007).
[19] T. Masuda, A. Zheludev, A. Bush, M. Markina, and A. Vasiliev, Phys. Rev. Lett. **92**, 177201 (2004).
[20] T. Masuda, A. Zheludev, B. Roessli, A. Bush, M. Markina, and A. Vasiliev, Phys. Rev. B **72**, 014405 (2005).
[21] H. J. Xiang and M.-H. Whangbo, Phys. Rev. Lett. **99**, 257203 (2007).
[22] S. W. Huang, D. J. Huang, J. Okamoto, C. Y. Mou, W. B. Wu, K. W. Yeh, C. L. Chen, M. K. Wu, H. C. Hsu, F. C. Chou, and C. T. Chen, Phys. Rev. Lett. **101**, 077205 (2008).
[23] D. Hüvonen, U. Nagel, T. Rõõm, Y. J. Choi, C. L. Zhang, S. Park, and S.-W. Cheong, Phys. Rev. B **80**, 100402(R) (2009).
[24] S. Seki, Y. Yamasaki, M. Soda, M. Matsuura, K. Hirota, and Y. Tokura, Phys. Rev. Lett. **100**, 127201 (2008).
[25] G. Lawes, M. Kenzelmann, N. Rogado, K. H. Kim, G. A. Jorge, R. J. Cava, A. Aharony, O. Entin-Wohlman, A. B. Harris, T. Yildirim, Q. Z. Huang, S. Park, C. Broholm, and A. P. Ramirez, Phys. Rev. Lett. **93**, 247201 (2004).
[26] G. Lawes, A. B. Harris, T. Kimura, N. Rogado, R. J. Cava, A. Aharony, O. Entin-Wohlman, T. Yildrim, M. Kenzelmann, C. Broholm, and A. P. Ramirez, Phys. Rev. Lett. **95**, 087205 (2005).
[27] A. B. Harris, T. Yildirim, A. Aharony, and O. Entin-Wohlman, Phys. Rev. B **73**, 184433 (2006).
[28] M. Uhrmacher, R. N. Attili, K. P. Lieb, K. Winzer, and M. Mekata, Phys. Rev. Lett. **76**, 4829 (1996).
[29] F. Ye, J. A. Fernandez-Baca, R. S. Fishman, Y. Ren, H. J. Kang, Y. Qiu, and T. Kimura, Phys. Rev. Lett. **99**, 157201 (2007).
[30] F. Wang and A. Vishwanath, Phys. Rev. Lett. **100**, 077201 (2008).
[31] J. T. Haraldsen, M. Swanson, G. Alvarez, and R. S. Fishman, Phys. Rev. Lett. **102**, 237204 (2009).
[32] T. Nakajima, S. Mitsuda, K. Takahashi, M. Yamano, K. Masuda, H. Yamazaki, K. Prokes, K. Kiefer, S. Gerischer, N. Terada, H. Kitazawa, M. Matsuda, K. Kakurai, H. Kimura, Y. Noda, M. Soda, M. Matsuura, and K. Hirota, Phys. Rev. B **79**, 214423 (2009).
[33] G. Quirion, M. L. Plumer, O. A. Petrenko, G. Balakrishnan, and C. Proust, Phys. Rev. B **80**, 064420 (2009).
[34] T. T. A. Lummen, C. Strohm, H. Rakoto, and P. H. M. van Loosdrecht, Phys. Rev. B **81**, 224420 (2010).
[35] S. Seki, Y. Onose, and Y. Tokura, Phys. Rev. Lett. **101**, 067204 (2008).
[36] K. Kimura, H. Nakamura, S. Kimura, M. Hagiwara, and T. Kimura, Phys. Rev. Lett. **103**, 107201 (2009).
[37] H. Yamaguchi, S. Ohtomo, S. Kimura, M. Hagiwara, K. Kimura, T. Kimura, T. Okuda, and K. Kindo, Phys. Rev. B **81**, 033104 (2010).
[38] T. Arnold, D. J. Payne, A. Bourlange, J. P. Hu, R. G. Egdell, L. F. J. Piper, L. Colakerol, A. DeMasi, P.-A. Glans, T. Learmonth, K. E. Smith, J. Guo, D. O. Scanlon, A. Walsh, B. J. Morgan, and G. W. Watson, Phys. Rev. B **79**, 075102 (2009).
[39] D. Shin, J. S. Foord, D. J. Payne, T. Arnold, D. J. Aston, R. G. Egdell, K. G. Godinho, D. O. Scanlon, B. J. Morgan, G. W. Watson, E. Mugnier, C. Yaicle, A. Rougier, L. Colakerol, P. A. Glans, L. F. J. Piper, and K. E. Smith, Phys. Rev. B **80**, 233105 (2009).
[40] K. Kimura, T. Otani, H. Nakamura, Y. Wakabayashi, and T. Kimura, J. Phys. Soc. Jpn. **78**, 113710 (2009).

[41]H. Kadowaki, H. Kikuchi, and Y. Ajiro, J. Phys. Condens. Matter **2**, 4485 (1990).
[42]M. Poienar, F. Damay, C. Martin, V. Hardy, A. Maignan, and G. André, Phys. Rev. B **79**, 014412 (2009).
[43]M. Soda, K. Kimura, T. Kimura, M. Matsuura, and K. Hirota, J. Phys. Soc. Jpn. **78**, 124703 (2009).
[44]M. Soda, K. Kimura, T. Kimura, and K. Hirota, Phys. Rev. B **81**, 100406(R) (2010).
[45]M. Frontzek, G. Ehlers, A. Podlesnyak, H. Cao, M. Matsuda, O. Zaharko, N. Aliouane, S. Barilo, and S. V. Shiryaev, (2011) e-print arXiv:1109.1747 [cond-mat.mtrl-sci].
[46]R. Kajimoto, K. Nakajima, S. Ohira-Kawamura, Y. Inamura, K. Kakurai, M. Arai, T. Hokazono, S. Oozono, and T. Okuda, J. Phys. Soc. Jpn. **79**, 123705 (2010).
[47]M. Poienar, F. Damay, C. Martin, J. Robert, and S. Petit, Phys. Rev. B **81**, 104411 (2010).
[48]T. Kimura, J. C. Lashley, and A. P. Ramirez, Phys. Rev. B **73**, 220401(R) (2006).
[49]S. Seki, Y. Yamasaki, Y. Shiomi, S. Iguchi, Y. Onose, and Y. Tokura, Phys. Rev. B **75**, 100403(R) (2007).
[50]J. T. Haraldsen and R. S. Fishman, Phys. Rev. B **82**, 144441 (2010).
[51]B. Kundys, A. Maignan, D. Pelloquin, and C. Simon, Solid State Sci. **11**, 1035 (2009).
[52]T. Nakajima, S. Mitsuda, S. Kanetsuki, K. Prokes, A. Podlesnyak, H. Kimura, and Y. Noda, J. Phys. Soc. Jpn. **76**, 043709 (2007).
[53]K. Kimura, H. Nakamura, K. Ohgushi, and T. Kimura, Phys. Rev. B **78**, 140401(R) (2008).
[54]T. E. Mason, D. Abernathy, I. Anderson, J. Ankner, T. Egami, G. Ehlers, A. Ekkebus, G. Granroth, M. Hagen, K. Herwig, J. Hodges, C. Hoffmann, C. Horak, L. Horton, F. Klose, J. Larese, A. Mesecar, D. Myles, J. Neuefeind, M. Ohl, C. Tulk, X. L. Wang, and J. Zhao, Physica B **385–386**, 955 (2006).
[55]G. Ehlers, A. A. Podlesnyak, J. L. Niedziela, E. B. Iverson, and P. E. Sokol, Rev. Sci. Instrum. **82**, 085108 (2011).
[56]J. R. D. Copley and J. C. Cook, Chem. Phys. **292**, 447 (2003).
[57]R. T. Azuah, L. R. Kneller, Y. Qiu, P. L. W. Tregenna-Piggott, C. M. Brown, J. R. D. Copley, and R. M. Dimeo, J. Res. Natl. Inst. Stand. Technol. **114**, 341 (2009).
[58]R. S. Fishman, F. Ye, J. A. Fernandez-Baca, J. T. Haraldsen, and T. Kimura, Phys. Rev. B **78**, 140407(R) (2008).
[59]R. S. Fishman and S. Okamoto, Phys. Rev. B **81**, 020402(R) (2010).
[60]J. T. Haraldsen and R. S. Fishman, J. Phys. Condens. Matter **21**, 216001 (2009).
[61]M. E. Zhitomirsky and I. A. Zaliznyak, Phys. Rev. B **53**, 3428 (1996).
[62]J. T. Haraldsen, F. Ye, R. S. Fishman, J. A. Fernandez-Baca, Y. Yamaguchi, K. Kimura, and T. Kimura, Phys. Rev. B **82**, 020404(R) (2010).
[63]R. S. Fishman, J. Phys.: Condens. Matter **23**, 366002 (2011).
[64]M. L. Plumer, Phys. Rev. B **76**, 144411 (2007).